



OPEN ACCESS

EDITED BY

Loïc Leclercq,
Université de Lille, France

REVIEWED BY

Sushobhan Mukhopadhyay,
University of Florida, United States
Manavi Yadav,
New Jersey Institute of Technology,
United States

*CORRESPONDENCE

Dawood Elhamifar,
✉ d.elhamifar@yu.ac.ir

RECEIVED 08 June 2023

ACCEPTED 17 August 2023

PUBLISHED 06 September 2023

CITATION

Neysi M and Elhamifar D (2023), Yolk-shell structured magnetic mesoporous organosilica supported ionic liquid/Cu complex: an efficient nanocatalyst for the green synthesis of pyranopyrazoles. *Front. Chem.* 11:1235415. doi: 10.3389/fchem.2023.1235415

COPYRIGHT

© 2023 Neysi and Elhamifar. This is an open-access article distributed under the terms of the [Creative Commons Attribution License \(CC BY\)](https://creativecommons.org/licenses/by/4.0/). The use, distribution or reproduction in other forums is permitted, provided the original author(s) and the copyright owner(s) are credited and that the original publication in this journal is cited, in accordance with accepted academic practice. No use, distribution or reproduction is permitted which does not comply with these terms.

Yolk-shell structured magnetic mesoporous organosilica supported ionic liquid/Cu complex: an efficient nanocatalyst for the green synthesis of pyranopyrazoles

Maryam Neysi and Dawood Elhamifar*

Department of Chemistry, Yasouj University, Yasouj, Iran

The preparation of yolk-shell structured magnetic mesoporous composites is a significant subject between researchers. Especially, modification of these composites with ionic liquid/metal complex is very important for catalytic processes. In the present study, a novel magnetic methylene-based periodic mesoporous organosilica (PMO)-supported ionic liquid/Cu complex with yolk-shell structure (YS-Fe₃O₄@PMO/IL-Cu) was prepared via the soft template-assisted method. The TGA, FT-IR, SEM, EDX, XRD, VSM, nitrogen-sorption, and ICP techniques were employed to identify YS-Fe₃O₄@PMO/IL-Cu. The YS-Fe₃O₄@PMO/IL-Cu material was applied as a powerful nanocatalyst for the synthesis of pyranopyrazoles under ultrasonic media. The study demonstrated that the YS-Fe₃O₄@PMO/IL-Cu nanocatalyst is highly recyclable, selective, and effective. The leaching test was performed to investigate the nature of the designed catalyst under the applied conditions.

KEYWORDS

periodic mesoporous organosilica, yolk-shell structure, ionic liquid, nanocomposite, pyranopyrazoles

1 Introduction

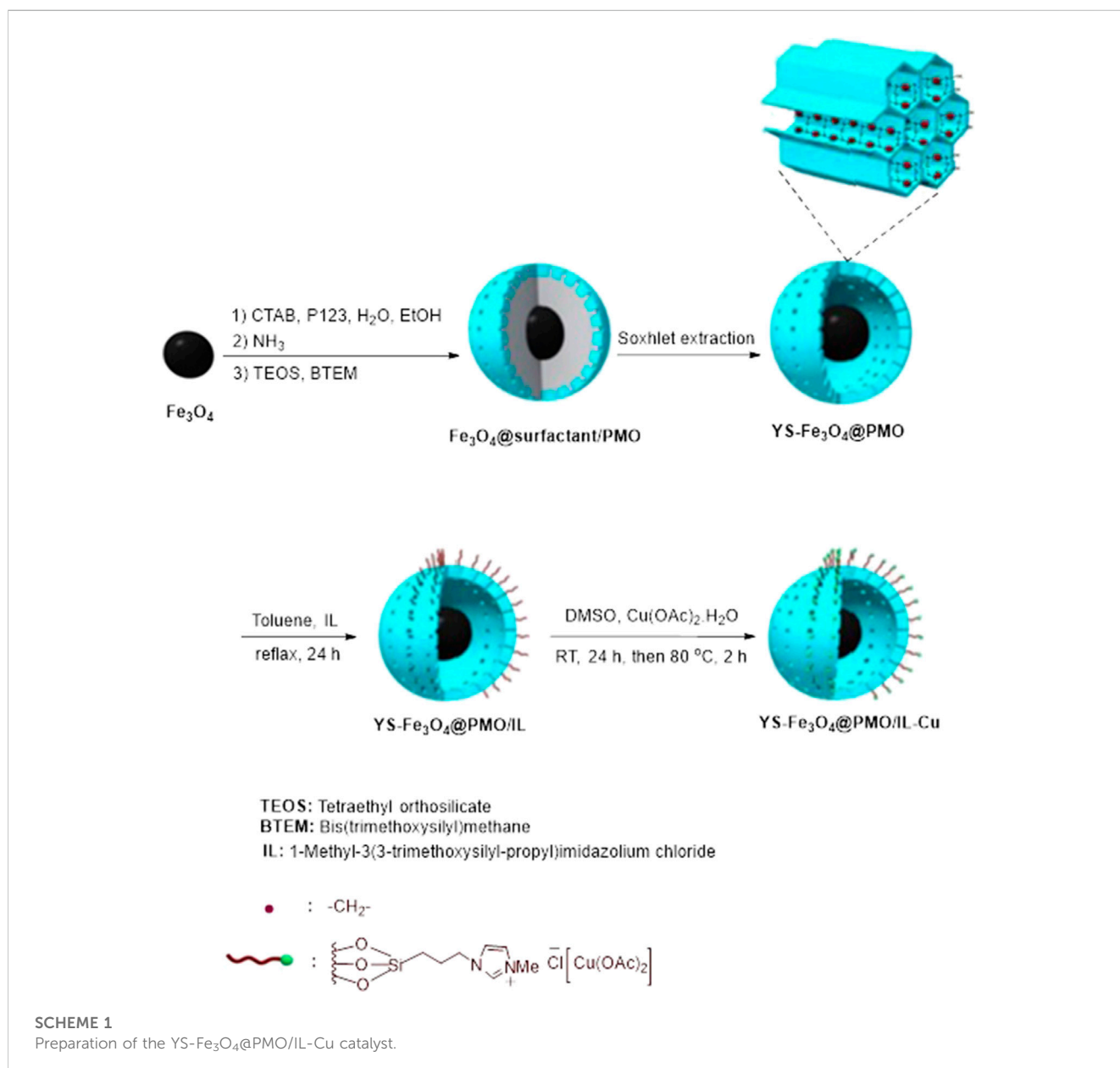
Yolk-shell structured nanoparticles (NPs) are hybrid materials in which a core is encapsulated in a hollow shell and can move freely within this shell, commonly demonstrated as core/void/shell. In this structure, the core is not blocked and thus provides an effective active site for the chemical processes (Kim et al., 2002; Kamata et al., 2003; Yin et al., 2004; Gao et al., 2007; Liu et al., 2013; Purbia and Paria, 2016; Xie et al., 2017). The unique properties of yolk-shell structured materials, such as low density, high surface area, permeable shells, high thermal stability, and interstitial hollow spaces, make them powerful platforms for biotechnology/biomedicine, controlled release, magnetic resonance imaging, data storage, catalysis, environmental remediation, etc. (Kresge et al., 1992; Vartuli et al., 1994; Holmes et al., 1998; Vartuli et al., 1998; Tsuji et al., 1999; Morishita et al., 2006; Puangnam and Unob, 2008; Du and He, 2011; Zhao et al., 2011; Ghaedi et al., 2013; Zhang, 2013; Nasab and Kiasat, 2016; Purbia and Paria, 2016). Among the various categories of yolk-shells (YSs), magnetic composites with Fe₃O₄ cores and nano-silica shells are very attractive due to their advantages such as good magnetic properties, high chemical

and thermal stability, non-toxicity, high adsorption capacity, high surface area, high biocompatibility, and high accessibility of -OH groups on their surface for any modification (Arruebo et al., 2006; Liu et al., 2011; Yang et al., 2015). Recently, the catalytic application of YS-structured magnetic mesoporous silica nanocomposites has received much attention. Some of the newly developed systems in this regard are Au@Void@PMO (Yang et al., 2015), Fe₃O₄@SiO₂@Pd/HSPMO (Dai et al., 2017), PMO-MHS (Zhang et al., 2008), and Fe₃O₄@void@mSiO₂ (Qiu et al., 2015).

Periodic mesoporous organosilica (PMOs), a desirable class of organic-inorganic composite materials with great properties such as high surface area, high lipophilicity, and high thermal and mechanical stability, have emerged as an ideal support (Wang et al., 2015; Yu et al., 2019; Norouzi et al., 2020; Neysi and Elhamifar, 2023). In particular, bifunctional PMOs (BPMOs), which contain organic functionalities on both the mesoporous walls and channels, are highly attractive for catalytic processes

On the other hand, ionic liquids (ILs) have attracted tremendous attention in chemistry and materials science in the last decade owing to their unique characteristics, such as low vapor pressure, high chemical and thermal stability, and their capability to dissolve a variety of compounds. In particular, recently, imidazolium-based ILs have been widely used as linkers for the effective immobilization of catalytic active sites on solid supports (Neysi et al., 2020; Jangra et al., 2021; Veysipour et al., 2021; Neysi and Elhamifar, 2022).

The preparation of pyranopyrazole derivatives has emerged as a powerful tool in organic synthesis because they are an important class of biologically active compounds. Some biological properties of pyranopyrazoles are anticancer, antifungal, anti-anxiety, antiviral, and anti-AIDS (Babaie and Sheibani, 2011; Moosavi-Zare et al., 2013; Zolfigol et al., 2013; Ali et al., 2014; Gujar et al., 2014; Pandit et al., 2015). To date, many homogeneous and heterogeneous catalysts have been reported for the synthesis of pyranopyrazoles under different conditions. However, some of these systems suffer from the problems of



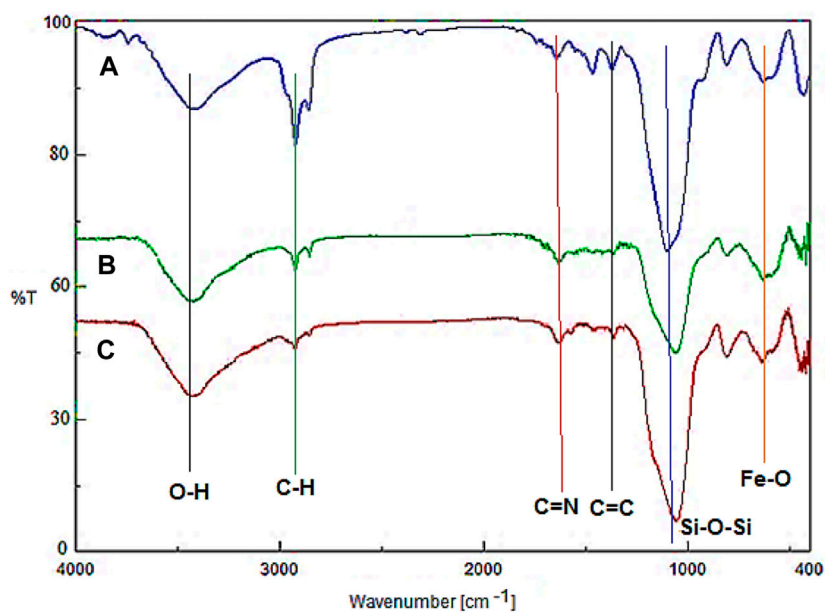


FIGURE 1
FT-IR of (A) Fe_3O_4 @Surfactants@PMO, (B) $\text{YS-Fe}_3\text{O}_4$ @PMO, and (C) $\text{YS-Fe}_3\text{O}_4$ @PMO/IL-Cu.

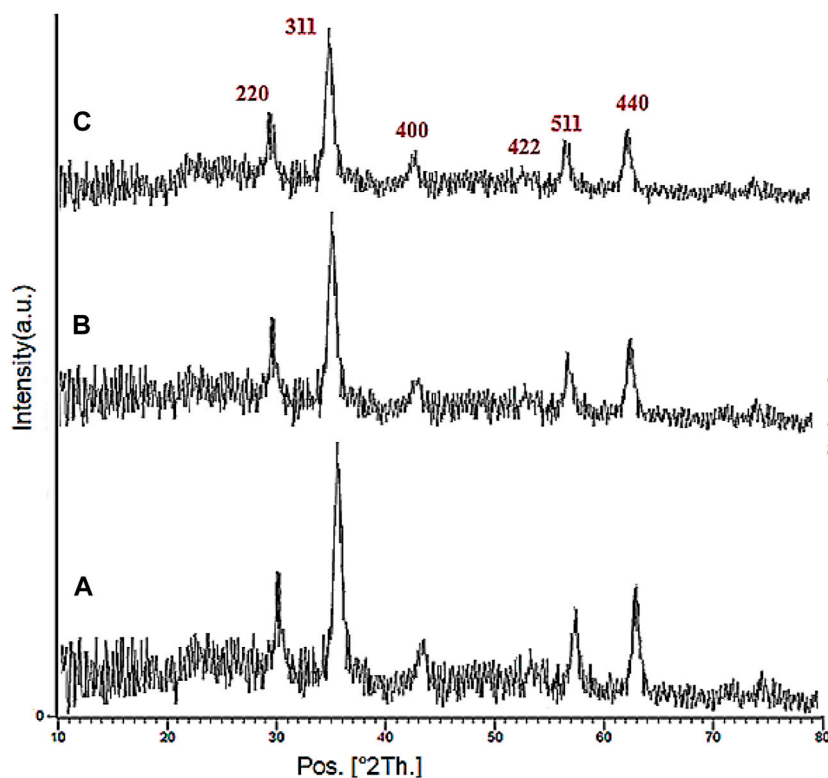
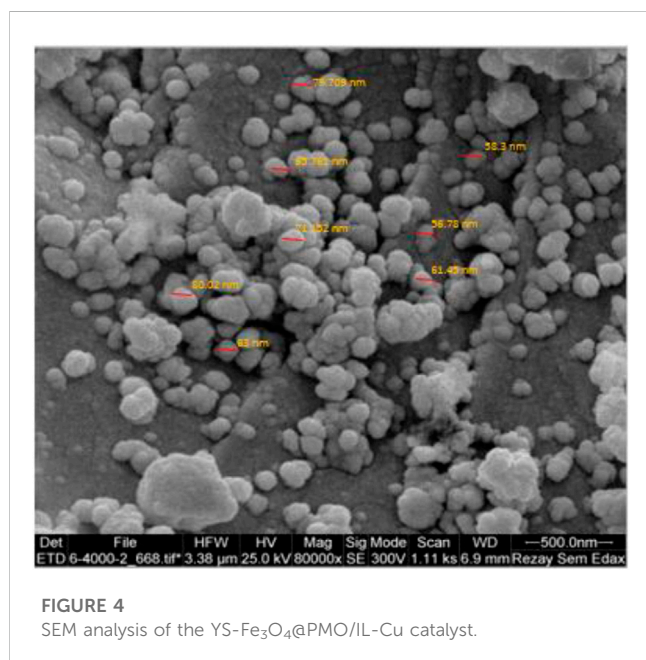
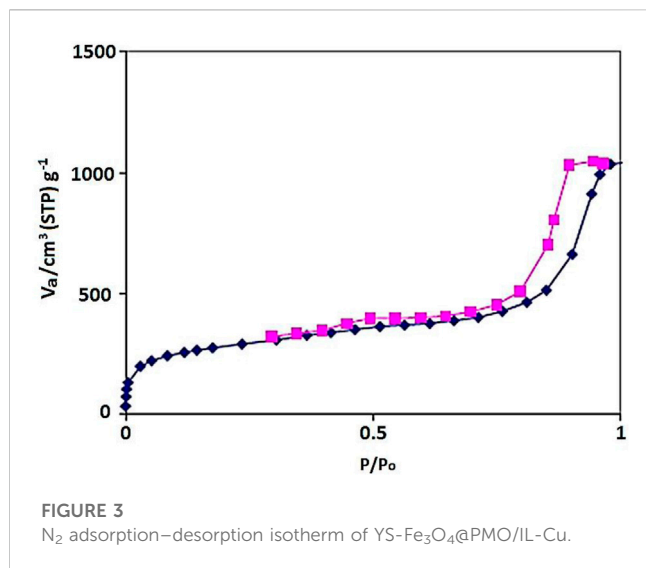


FIGURE 2
PXRD pattern of (A) Fe_3O_4 , (B) $\text{YS-Fe}_3\text{O}_4$ @PMO, and (C) $\text{YS-Fe}_3\text{O}_4$ @PMO/IL-Cu.

high catalyst loading, harsh conditions, and the use of toxic organic solvents. Therefore, design a green and efficient catalytic system to overcome the above limitations is a significant subject between

chemists. Given the above and continuing our recent studies on the design and preparation of novel magnetic and mesoporous catalytic systems, herein novel magnetic methylene and ionic liquid-based



bifunctional periodic mesoporous organosilica (BPMO) supported copper with yolk-shell structure (YS-Fe₃O₄@PMO/IL-Cu) was prepared and applied as an effective and recoverable catalyst for the synthesis of pyranopyrazoles under green conditions. In this BPMO, methylene functional groups are incorporated into the mesoporous walls, while ionic liquid functions are located in the mesoporous channels.

2 Experimental section

2.1 Synthesis of YS-Fe₃O₄@PMO NPs

For the synthesis of YS-Fe₃O₄@PMO, Fe₃O₄ NPs were first prepared according to our previous procedure (Neysi et al., 2019). Then, Fe₃O₄ NPs (0.25 g) were added to a reaction flask containing

EtOH)16 mL, H₂O (36 mL), CTAB (0.72 g), pluronic P123 (17.1 g) and ammonia solution (0.9 mL, 25% wt). This was stirred at 35°C–40°C for 0.5 h. Next, tetraethyl orthosilicate (TEOS, 0.7 g) and bis(triethoxysilyl)methane (BTEM, 2.1 g) were added to the reaction flask, and stirring continued for 1 h. The resulting mixture was statically heated at 100°C for 17 h. The product was separated, washed with ethanol and water, and dried at 80°C for 7 h. Finally, to obtain a yolk-shell structure, the CTAB and pluronic P123 templates were removed by Soxhlet extraction (Zhang et al., 2008).

2.2 Synthesis of YS-Fe₃O₄@PMO/IL NPs

For this part of the study, YS-Fe₃O₄@PMO NPs (0.25 g) were added and ultrasonically dispersed in toluene (20 mL) at RT for 20 min. Then, 1-methyl-3-(3-trimethoxysilylpropyl) imidazolium chloride (0.15 g) was added, and the resulting mixture was refluxed under Ar atmosphere for 1 day. After cooling to room temperature, the product was collected using a magnet, washed with ethanol, dried at 75°C for 11 h, and named YS-Fe₃O₄@PMO/IL.

2.3 Synthesis of YS-Fe₃O₄@PMO/IL-Cu catalyst

First, the YS-Fe₃O₄@PMO/IL NPs (0.25 g) were sonicated in DMSO (40 mL) for 20 min. Then, Cu(OAc)₂·4H₂O (0.75 g) was added while stirring at RT for 1 day. The resulting mixture was then stirred at 80°C for 2 h. The product was collected using a magnet, washed with ethanol and H₂O, dried at 75°C for 11 h, and named YS-Fe₃O₄@PMO/IL-Cu (Elhamifar et al., 2017). According to the ICP analysis, the loading of copper on the designed material was found to be 0.45 mmol Cu/g of YS-Fe₃O₄@PMO/IL-Cu.

2.4 Synthesis of pyranopyrazoles using YS-Fe₃O₄@PMO/IL-Cu catalyst

For this part of the study, YS-Fe₃O₄@PMO/IL-Cu catalyst (0.36 mol%) was added to a flask containing aldehyde (1 mmol), malononitrile (1 mmol), ethyl acetoacetate (1 mmol), and hydrazine hydrate (1 mmol). The reaction progress was monitored under ultrasonic conditions at RT. After the reaction was completed, the hot EtOH was added to the reaction flask, and YS-Fe₃O₄@PMO/IL-Cu was separated using an external magnetic field. The pure pyranopyrazoles were obtained after recrystallizing the crude mixture in EtOH.

2.5 IR, ¹H and ¹³C-NMR data of pyranopyrazoles

2.5.1 6-Amino-4-(2,4-dichlorophenyl)-3-methyl-1,4-dihydropyranopyrazole-5-carbonitrile

IR (KBr, cm⁻¹): 3,480 (NH), 3,253, 3,118 (NH₂), 3,075 (=C-H stretching vibration, sp²), 2,927 (C-H stretching vibration, sp³), 2,184 (CN), 1,641 (C=N), 1,467 (C=C), 1,411 (C-O, ether), 869 (C-Cl). ¹H-NMR (400 MHz, CDCl₃): δ (ppm), 1.90 (s, 3H), 4.45 (s,

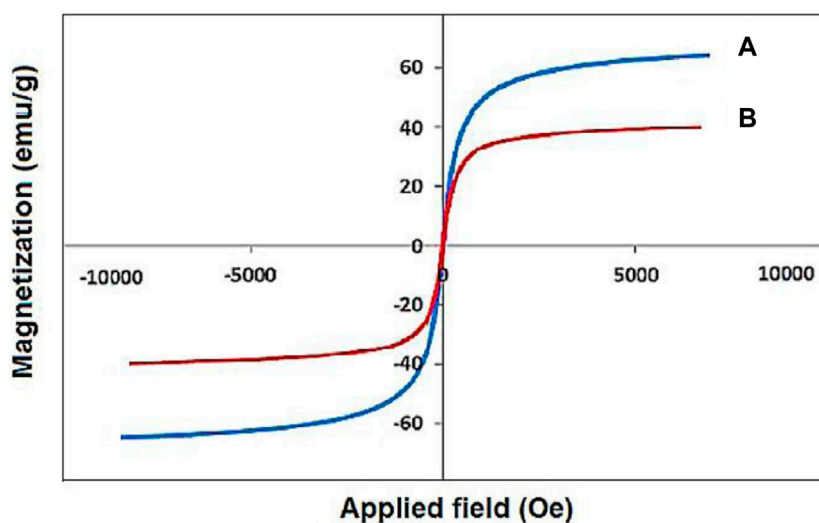


FIGURE 5
The VSM analysis of (A) Fe_3O_4 and (B) $\text{YS-Fe}_3\text{O}_4@PMO/IL-Cu$.

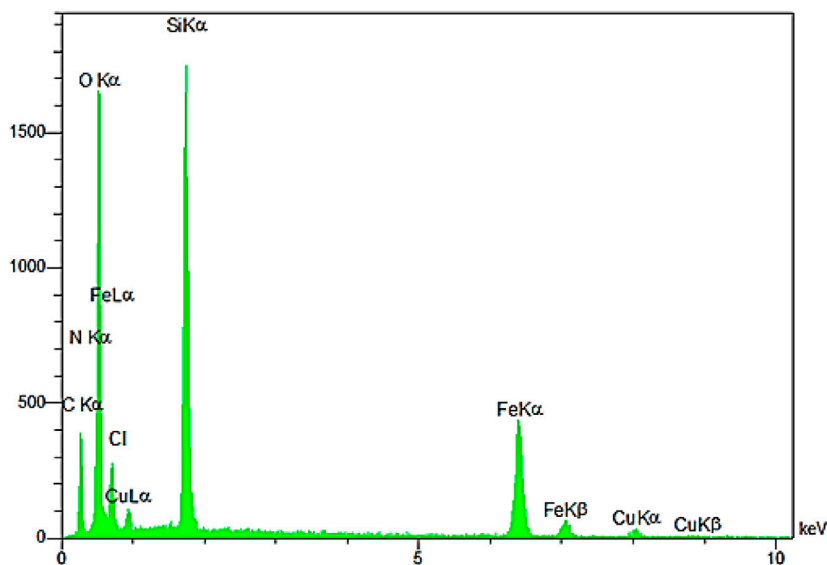


FIGURE 6
The EDX analysis of the $\text{YS-Fe}_3\text{O}_4@PMO/IL-Cu$ catalyst.

1H), 7.01 (d, 1H, $j = 8$ Hz), 7.11 (d, 1H, $j = 8$ Hz), 7.76 (s, 1H), 8.60 (s, 2H, NH_2), 11.95 (s, 1H, NH). $^{13}\text{C-NMR}$ (100 MHz, CDCl_3): δ (ppm) 13.2, 16, 59.3, 110.0, 117.4, 126.7, 130.0, 131.0, 132.4, 135.0, 139.6, 142.6, 163.7, 177.4.

2.5.2 6-Amino-4-(2-bromo-6-hydroxyphenyl)-3-methyl-1,4-dihydropyrano[2,3-*c*]pyrazole-5-carbonitrile

IR (KBr, cm^{-1}): 3,495 (OH), 3,380 (NH), 3,255, 3,120 (NH_2), 3,079 ($=\text{C-H}$ stretching vibration, sp^2), 2,917 (C-H stretching vibration, sp^3), 2,187 (CN), 1,619 ($\text{C}=\text{N}$), 1,475 ($\text{C}=\text{C}$), 1,268 (C-O , ether), 823

(C-Br). $^1\text{H-NMR}$ (400 MHz, CDCl_3): δ (ppm) 1.94 (s, 3H), 4.53 (s, 1H), 5.30 (s, 1H, OH), 6.92 (t, 1H, $j = 5.8$ Hz), 7.10 (d, 1H, $j = 8$ Hz), 7.11 (d, 1H, $j = 8$ Hz), 8.67 (s, 2H, NH_2), 11.88 (s, 1H, NH). $^{13}\text{C-NMR}$ (100 MHz, CDCl_3): δ (ppm), 13.3, 16.5, 59.5, 110.2, 113.4, 117.3, 123.7, 123.9, 128.7, 128.9, 139.6, 156.6, 163.9, 177.6.

3 Results and discussion

The synthesis of $\text{YS-Fe}_3\text{O}_4@PMO/IL-Cu$ NPs is presented in Scheme 1. Initially, the surface of Fe_3O_4 NPs was coated with a

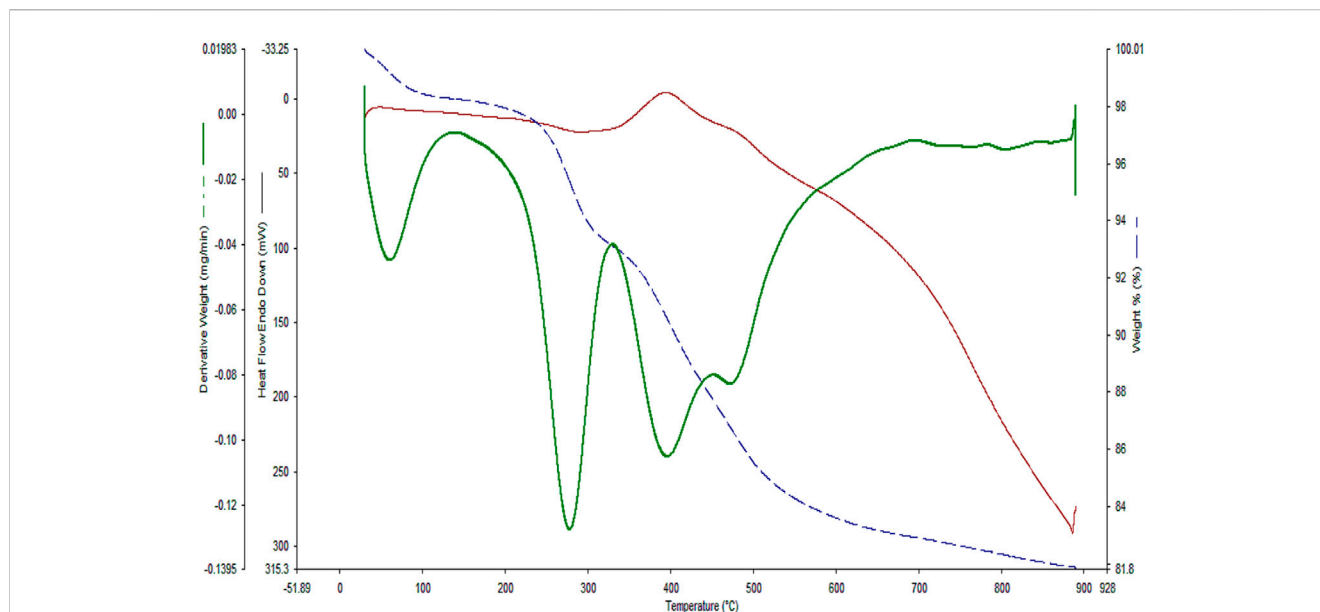


FIGURE 7
The TG analysis of the YS-Fe₃O₄@PMO/IL-Cu catalyst.

TABLE 1 Effect of solvent and catalyst loading in the synthesis of dihydropyrano[2, 3-*c*]pyrazole^a.

Entry	Solvent	Catalyst (mol%)	Yield (%)
1	—	YS-Fe ₃ O ₄ @PMO/IL-Cu (0.36)	28
2	EtOH	YS-Fe ₃ O ₄ @PMO/IL-Cu (0.36)	65
3	CH ₃ CN	YS-Fe ₃ O ₄ @PMO/IL-Cu (0.36)	14
4	DMF	YS-Fe ₃ O ₄ @PMO/IL-Cu (0.36)	50
5	<i>n</i> -Hexane	YS-Fe ₃ O ₄ @PMO/IL-Cu (0.36)	<10
6 ^b	H ₂ O	YS-Fe ₃ O ₄ @PMO/IL-Cu (0.36)	95
7	H ₂ O	YS-Fe ₃ O ₄ @PMO/IL-Cu (0.45)	95
8	H ₂ O	YS-Fe ₃ O ₄ @PMO/IL-Cu (0.18)	68
9	H ₂ O	YS-Fe ₃ O ₄ @PMO/IL-Cu (0.09)	35
10	H ₂ O	YS-Fe ₃ O ₄ @PMO/IL (0.008 g)	23
11	H ₂ O	YS-Fe ₃ O ₄ @PMO (0.008 g)	21
12	H ₂ O	Fe ₃ O ₄ (0.008 g)	35

^aAll reactions were performed at RT, for 10 min.

^bOptimum conditions.

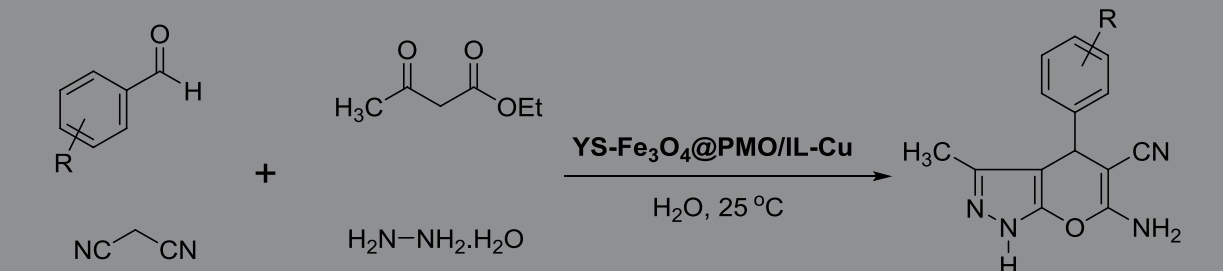
periodic mesoporous organosilica shell via hydrolysis and co-condensation of TEOS and BTEM in the presence of CTAB and pluronic P123 surfactants. To obtain a yolk-shell structure, the CTAB and pluronic P123 templates were removed by Soxhlet extraction. Subsequently, the surface of YS-Fe₃O₄@PMO/IL NPs was modified

with a complex of ionic liquid and copper salt to obtain YS-Fe₃O₄@PMO/IL-Cu catalyst. It is important to note that the YS-Fe₃O₄@PMO/IL-Cu catalyst is a multifunctional material that contains the advantages of magnetic NPs, supported ionic liquids and YS-structured mesoporous materials. For example, as shown in Scheme 1, IL moieties play a key role in the immobilization and stabilization of catalytic copper species.

Figure 1 demonstrates the FT-IR of Fe₃O₄@surfactants@PMO, YS-Fe₃O₄@PMO, and YS-Fe₃O₄@PMO/IL-Cu NPs. For all samples, the peaks observed at 588 and 3300–3450 cm⁻¹ are related to Fe-O and O-H bonds, respectively. Also, the signals observed at 823 and 1078 cm⁻¹ are assigned to the asymmetric and symmetric vibrations of the Si-O-Si bond, respectively (Figures 1A,B). It should be noted that before surfactant extraction, the sharp peaks at 2923 and 2855 cm⁻¹ are due to C-H stretching vibrations of CTAB and P123 (Figure 1A). After the Soxhlet extraction, the intensity of these peaks is significantly decreased, confirming the successful elimination of surfactants (Figure 1B). In Figure 1C, the peaks at 1418 and 1625 cm⁻¹ are related to C=C and C=N of imidazolium rings, respectively.

The XRD analysis of the Fe₃O₄, YS-Fe₃O₄@PMO, and YS-Fe₃O₄@PMO/IL-Cu catalysts is displayed in Figure 2. This clearly illustrates six signals at 2 Θ = 30.3, 35.7, 43.4, 53.8, 57.7, and 63.0°, which is in agreement with the standard XRD pattern of Fe₃O₄ NPs. This confirms that the Fe₃O₄ NPs are very stable during the preparation of the YS-Fe₃O₄@PMO/IL-Cu catalyst. It is also important to note that for YS-Fe₃O₄@PMO and YS-Fe₃O₄@PMO/IL-Cu materials, the intensity of PXRD peaks is decreased, indicating the successful modification of magnetite NPs with Me-PMO, IL, and copper moieties. (Figure 2).

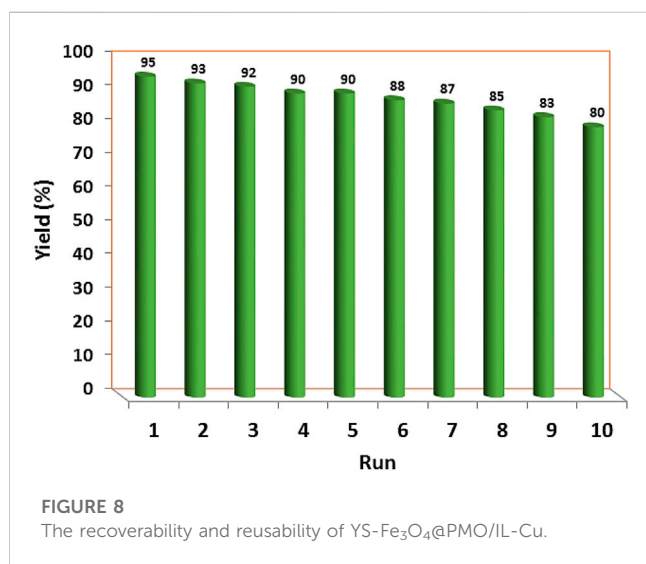
The N₂ adsorption–desorption isotherm of the YS-Fe₃O₄@PMO/IL-Cu showed a type IV isotherm with an H1 hysteresis loop, which is characteristic of ordered mesostructures with high regularity (Figure 3). Also, the BET surface area, average pore

TABLE 2 Synthesis of pyranopyrazoles by using YS-Fe₃O₄@PMO/IL-Cu^a.


Entry	Aldehyde	Time (min)	Yield (%) ^b	Found M. P.	Reported M. P.
1	C ₆ H ₅ CHO	10	95	241–243	240–243 ³³
2	4-MeO-C ₆ H ₄ CHO	15	89	206–208	206–209 ³³
3	4-Me-C ₆ H ₄ CHO	20	89	174–176	176–177 ²⁸
4	3-HO-C ₆ H ₄ CHO	17	90	262–264	260–262 ³³
5	4-Br-C ₆ H ₄ CHO	12	89	182–184	180–182 ³³
6	4-CN-C ₆ H ₄ CHO	10	96	197–199	196–198 ³⁰
7	4-NO ₂ -C ₆ H ₄ CHO	10	87	191–193	194–196 ²⁸
8	4-Cl-C ₆ H ₄ CHO	8	93	231–233	233–235 ³²
9	2,4-diCl-C ₆ H ₃ CHO	25	85	217–219	New
10	2-Br-6-HO-C ₆ H ₃ CHO	50	86	271–273	New

^aConditions: ethyl acetoacetate (1 mmol), malononitrile (1 mmol), benzaldehyde (1 mmol), hydrazine hydrate (1 mmol), and catalyst (0.36 mol%) in H₂O (8 mL) at 25°C.

^bIsolated yields.



size, and total pore volume of the designed YS-Fe₃O₄@PMO/IL-Cu nanocomposite were found to be 659 m²/g, 7.6 nm, and 1.30 cm³/g, respectively. These results demonstrate the good formation of an ordered PMO shell for YS-Fe₃O₄@PMO/IL-Cu.

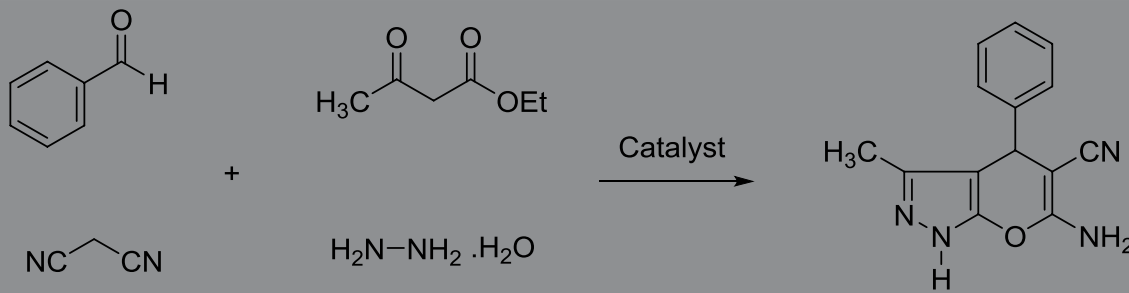
The SEM image of the YS-Fe₃O₄@PMO/IL-Cu catalyst showed the presence of uniform particles with spherical structure and an average size of 70 nm (Figure 4). These are very good NPs for catalytic and adsorption processes.

The VSM analysis showed a saturation magnetization of about 30 emu·g⁻¹ for the designed YS-Fe₃O₄@PMO/IL-Cu nanocatalyst, lower than that of pure magnetic iron oxide NPs (Figure 5) (Norouzi et al., 2020). This proves the successful coating of PMO shell on magnetite NPs and also confirms the high magnetic properties of the catalyst, which is an excellent characteristic in the catalytic field.

The EDX pattern confirmed the presence of the desired elements in the YS-Fe₃O₄@PMO/IL-Cu catalyst (Figure 6). This analysis illustrated the signals of C, Si, N, Cu, Fe, and O elements in the catalyst, proving the successful incorporation and immobilization of the expected inorganic and organic moieties into/onto Fe₃O₄ NPs.

In the next step, TGA analysis was conducted to evaluate the thermal stability of the YS-Fe₃O₄@PMO/IL-Cu catalyst (Figure 7). The first weight loss below 120°C is due to the loss of water and alcoholic solvents left over from the synthesis process. Another weight loss at 200°C–320°C is related to the decomposition of the remaining CTAB and P123 surfactants. The highest weight loss, observed at 325°C–650°C, is attributed to the removal of methylene and ionic liquid functional groups, which are incorporated/immobilized in/on the structure of YS-Fe₃O₄@PMO/IL-Cu nanocomposite.

After characterizing the YS-Fe₃O₄@PMO/IL-Cu catalyst, its application in the synthesis of dihydropyrano [2, 3-*c*]pyrazoles was investigated. For this part of the study, the condensation between malononitrile, PhCHO, ethyl acetoacetate, and hydrazine hydrate was selected as a model reaction. The

TABLE 3 Comparative study between the activity of the YS-Fe₃O₄@PMO/IL-Cu catalyst and several identified catalysts in the synthesis of pyranopyrazoles.


Entry	Catalyst	Conditions	Recovery numbers	Ref
1	L-proline	H ₂ O, cat. (10 mol%), reflux, 10 min	-	Mecadon et al. (2011)
2	SiO ₂ -TMG	Neat, cat. (10 mol%), 100°C, 30 min	4	Atar et al. (2014)
3	Fe ₃ O ₄ @SiO ₂ -HMTA-SO ₃ H	Solvent free, cat. (0.03 g), RT, 12 min	4	Ghorbani-Vaghei and Izadkhan (2018)
4	Fe ₃ O ₄ @SiO ₂ -EP-NH-HPA	H ₂ O, cat. (0.02 g), RT, 5 min	7	Hosseini Mohtasham and Gholizadeh (2020)
5	Fe ₃ O ₄	H ₂ O, cat. (0.015 g), RT, 60 min	8	Ali et al. (2014)
6	YS-Fe ₃ O ₄ @PMO/IL-Cu	H ₂ O, cat. (0.36 mol%), RT, 10 min	9	This work

effects of the solvent and catalyst loading were studied at RT under ultrasonic conditions. As displayed in Table 1, the effects of different solvents such as EtOH, CH₃CN, *n*-Hexane, DMF, H₂O, and solvent-free media were studied, and the best results were obtained in H₂O at 25°C (Table 1, entries 1–6). The effect of catalyst loading was also investigated, with the best yield obtained in the presence of 0.36 mol% of YS-Fe₃O₄@PMO/IL-Cu. According to these results, the use of 0.36 mol% of YS-Fe₃O₄@PMO/IL-Cu in H₂O at 25°C under ultrasonic irradiation was chosen as the optimum condition. In order to prove whether the copper centers act as catalytic sites or not, in the next study the reaction was carried out using Cu-free Fe₃O₄, YS-Fe₃O₄@PMO, and YS-Fe₃O₄@PMO/IL materials under the same conditions as YS-Fe₃O₄@PMO/IL-Cu (Table 1, entries 10–12). The result showed that for all Cu-free samples, only a low yield of the desired product was obtained, indicating that the reaction is mainly catalyzed by immobilized copper sites.

After optimizing the different parameters, the efficiency of the YS-Fe₃O₄@PMO/IL-Cu nanocatalyst was evaluated by using different aldehyde substrates for the preparation of pyrazole derivatives. As seen in Table 2, all investigated aldehydes were converted to their corresponding products in high yields. These results confirm the high efficiency of YS-Fe₃O₄@PMO/IL-Cu for the preparation of a wide range of biologically active pyranopyrazoles.

The recoverability and reusability of the YS-Fe₃O₄@PMO/IL-Cu catalyst were investigated in the condensation of malononitrile, ethyl acetoacetate, benzaldehyde, and hydrazine hydrate under optimized conditions. For this purpose, at the end of the reaction, the catalyst was magnetically removed, washed, and reused in the next run under the same conditions as in the first step. The results indicated that the synthesized catalyst can be recovered and reused at least 9 times without significant loss of efficiency (Figure 8).

A leaching test was then performed to investigate the nature of the catalyst under the reaction conditions. For this purpose, the model reaction was selected as the test. After about 50% of the process was completed, the catalyst was removed using an external magnet, and the reaction progress of the residue was monitored for 60 min. The result demonstrated no further progress of the reaction, confirming no leaching of the active catalytic species and also the heterogeneous nature of the designed catalyst. This result confirms the successful immobilization of the copper moieties on the material framework.

Next, a comparative study was performed between the activity of the YS-Fe₃O₄@PMO/IL-Cu catalyst and several identified catalysts in the synthesis of pyranopyrazoles (Table 3). The results showed that our designed catalyst is better than other catalysts in terms of catalyst loading, reaction time, and recovery numbers. These findings are attributed to the magnetic nature, mesoporous structure, supported ionic liquids, and high stability of the designed YS-Fe₃O₄@PMO/IL-Cu nanocatalyst.

4 Conclusion

In this study, the magnetic YS-Fe₃O₄@PMO/IL-Cu catalyst was prepared and identified by using PXRD, FT-IR, TGA, EDX, ICP, SEM, nitrogen sorption, and VSM analyses. The TGA, EDX, and FT-IR analyses demonstrated the high chemical and thermal stability of YS-Fe₃O₄@PMO/IL-Cu. The VSM and PXRD analyses showed very good magnetic properties of the material. The nano dimensions and particle size of this catalyst were confirmed using SEM analysis. The nitrogen-sorption diagram also showed a mesoporous structure for the designed catalyst. The YS-Fe₃O₄@PMO/IL-Cu nanocomposite was used as a powerful catalyst in the synthesis of biologically active

pyranopyrazoles, giving the desired products in high yields and selectivity. Moreover, the YS-Fe₃O₄@PMO/IL-Cu catalyst was easily recovered and reused at least 9 times without any significant decrease in its efficiency.

Data availability statement

The original contributions presented in the study are included in the article/supplementary material, further inquiries can be directed to the corresponding author.

Author contributions

MN investigation, writing–original draft. DE conceptualization, writing–review and editing, supervision,

References

- Ali, M. A. E. A., Remaily, E., and Mohamed, S. K. (2014). Eco-friendly synthesis of guanidyltetrazole compounds and 5-substituted 1H-tetrazoles in water under microwave irradiation. *Tetrahedron* 70, 270–275. doi:10.1016/j.tet.2013.11.069
- Arruebo, M., Galán, M., Navascués, N., Téllez, C., Marquina, C., Ibarra, M. R., et al. (2006). Development of magnetic nanostructured silica-based materials as potential vectors for drug-delivery applications. *Chem. Mater.* 18, 1911–1919. doi:10.1021/cm051646z
- Atar, A. B., Kim, J. T., Lim, K. T., and Jeong, Y. T. (2014). Synthesis of 6-amino-2, 4-dihydropyrano [2, 3-c] pyrazol-5-carbonitriles catalyzed by silica-supported tetramethylguanidine under solvent-free conditions. *Synth. Commun.* 44, 2679–2691. doi:10.1080/00397911.2014.913634
- Babaie, M., and Sheibani, H. (2011). Nanosized magnesium oxide as a highly effective heterogeneous base catalyst for the rapid synthesis of pyranopyrazoles via a tandem four-component reaction. *Arabian J. Chem.* 4, 159–162. doi:10.1016/j.arabjc.2010.06.032
- Dai, J., Zou, H., Wang, R., Wang, Y., Shi, Z., and Qiu, S. (2017). Yolk–shell Fe₃O₄@SiO₂@PMO: Amphiphilic magnetic nanocomposites as an adsorbent and a catalyst with high efficiency and recyclability. *Green Chem.* 19, 1336–1344. doi:10.1039/c6gc02926d
- Du, X., and He, J. (2011). Spherical silica micro/nanomaterials with hierarchical structures: Synthesis and applications. *Nanoscale* 3, 3984–4002. doi:10.1039/c1nr10660k
- Elhamifar, D., Mofatehnia, P., and Faal, M. (2017). Magnetic nanoparticles supported Schiff-base/copper complex: An efficient nanocatalyst for preparation of biologically active 3, 4-dihydropyrimidinones. *J. Colloid Interface Sci.* 504, 268–275. doi:10.1016/j.jcis.2017.05.044
- Gao, J., Liang, G., Zhang, B., Kuang, Y., Zhang, X., and Xu, B. (2007). FePt@CoS₂ yolk–shell nanocrystals as a potent agent to kill HeLa cells. *J. Am. Chem. Soc.* 129, 1428–1433. doi:10.1021/ja067785e
- Ghaedi, M., Elhamifar, D., Negintaji, G., and Banakar, M. H. (2013). Thiol functionalised ionic liquid based xerogel: A novel and efficient support for the solid phase extraction of transition metal ions. *Int. J. Environ. Anal. Chem.* 93, 1525–1536. doi:10.1080/03067319.2013.814118
- Ghorbani-Vaghei, R., and Izadkhah, V. (2018). Preparation and characterization of hexamethylenetetramine-functionalized magnetic nanoparticles and their application as novel catalyst for the synthesis of pyranopyrazole derivatives. *Appl. Organomet. Chem.* 32, e4025. doi:10.1002/aoc.4025
- Gujar, J. B., Chaudhari, M. A., Kawade, D. S., and Shingare, M. S. (2014). Molecular sieves: An efficient and reusable catalyst for multi-component synthesis of dihydropyrano [2, 3-c] pyrazole derivatives. *Tetrahedron Lett.* 55, 6030–6033. doi:10.1016/j.tetlet.2014.08.127
- Holmes, S. M., Zholobenko, V. L., Thursfield, A., Plaisted, R. J., Cundy, C. S., and Dwyer, J. (1998). *In situ* FTIR study of the formation of MCM-41. *J. Chem. Soc. Faraday Trans.* 94, 2025–2032. doi:10.1039/a801898g
- Hosseini Mohtasham, N., and Gholizadeh, M. (2020). Nano silica extracted from horsetail plant as a natural silica support for the synthesis of H3PW12O40 immobilized on aminated magnetic nanoparticles (Fe₃O₄@SiO₂-EP-NH-HPA): A novel and efficient heterogeneous nanocatalyst for the green one-pot synthesis of pyrano [2, 3-c] pyrazole derivatives. *Res. Chem. Intermed.* 46, 3037–3066. doi:10.1007/s11164-020-04133-8
- Jangra, A., Kumar, P., Khanna, R., Chaudhary, A., Kumar, S., Singh, J., et al. (2021). A brief and specific review on the utility of surface functionalized magnetite nanoparticles for the removal of dye from contaminated water. *Rasayan J. Chem.* 14, 829–835. doi:10.31788/rjc.2021.1426207
- Kamata, K., Lu, Y., and Xia, Y. (2003). Synthesis and characterization of monodispersed core–shell spherical colloids with movable cores. *J. Am. Chem. Soc.* 125, 2384–2385. doi:10.1021/ja0292849
- Kim, M., Sohn, K., Na, H. B., and Hyeon, T. (2002). Synthesis of nanorattles composed of gold nanoparticles encapsulated in mesoporous carbon and polymer shells. *Nano Lett.* 2, 1383–1387. doi:10.1021/nl025820j
- Kresge, A. C., Leonowicz, M., Roth, W. J., Vartuli, J., and Beck, J. (1992). Ordered mesoporous molecular sieves synthesized by a liquid-crystal template mechanism. *Nature* 359, 710–712. doi:10.1038/359710a0
- Liu, J., Qiao, S. Z., Chen, J. S., Lou, X. W. D., Xing, X., and Lu, G. Q. M. (2011). Yolk/shell nanoparticles: New platforms for nanoreactors, drug delivery and lithium-ion batteries. *Chem. Commun.* 47, 12578–12591. doi:10.1039/c1cc13658e
- Liu, J., Xu, J., Che, R., Chen, H., Liu, M., and Liu, Z. (2013). Hierarchical Fe₃O₄@TiO₂ yolk–shell microspheres with enhanced microwave-absorption properties. *Chemistry–A Eur. J.* 19, 6746–6752. doi:10.1002/chem.201203557
- Mecadon, H., Rohman, M. R., Rajbangshi, M., and Myrboh, B. (2011). γ -Alumina as a recyclable catalyst for the four-component synthesis of 6-amino-4-alkyl/aryl-3-methyl-2, 4-dihydropyrano [2, 3-c] pyrazole-5-carbonitriles in aqueous medium. *Tetrahedron Lett.* 52, 2523–2525. doi:10.1016/j.tetlet.2011.03.036
- Moosavi-Zare, A. R., Zolfogol, M. A., Noroozizadeh, E., Tavasoli, M., Khakyzadeh, V., and Zare, A. (2013). Synthesis of 6-amino-4-(4-methoxyphenyl)-5-cyano-3-methyl-1-phenyl-1, 4-dihydropyrano [2, 3-c] pyrazoles using disulfonic acid imidazolium chloroaluminate as a dual and heterogeneous catalyst. *New J. Chem.* 37, 4089–4094. doi:10.1039/c3nj00629h
- Morishita, M., Shiraishi, Y., and Hirai, T. (2006). Ti-containing mesoporous organosilica as a photocatalyst for selective olefin epoxidation. *J. Phys. Chem. B* 110, 17898–17905. doi:10.1021/jp062355w
- Nasab, M. J., and Kiasat, A. R. (2016). Multifunctional Fe₃O₄@nSiO₂@mSiO₂/Pr-Imi-NH₂: Ag core–shell microspheres as highly efficient catalysts in the aqueous reduction of nitroarenes: Improved catalytic activity and facile catalyst recovery. *Rsc Adv.* 6, 41871–41877. doi:10.1039/c6ra00120c
- Neysi, M., and Elhamifar, D. (2023). Magnetic ethylene-based periodic mesoporous organosilica supported palladium: An efficient and recoverable nanocatalyst for Suzuki reaction. *Front. Chem.* 11, 1112911. doi:10.3389/fchem.2023.1112911
- Neysi, M., Elhamifar, D., and Norouzi, M. (2020). Ionic liquid functionalized magnetic organosilica nanocomposite: A powerful and efficient support for manganese catalyst. *Mater. Chem. Phys.* 243, 122589. doi:10.1016/j.matchemphys.2019.122589
- Neysi, M., and Elhamifar, D. (2022). Pd-containing magnetic periodic mesoporous organosilica nanocomposite as an efficient and highly recoverable catalyst. *Sci. Rep.* 12, 7970. doi:10.1038/s41598-022-11918-x

visualization. All authors contributed to the article and approved the submitted version.

Conflict of interest

The authors declare that the research was conducted in the absence of any commercial or financial relationships that could be construed as a potential conflict of interest.

Publisher's note

All claims expressed in this article are solely those of the authors and do not necessarily represent those of their affiliated organizations, or those of the publisher, the editors and the reviewers. Any product that may be evaluated in this article, or claim that may be made by its manufacturer, is not guaranteed or endorsed by the publisher.

- Neysi, M., Zarnegaryan, A., and Elhamifar, D. (2019). Core-shell structured magnetic silica supported propylamine/molybdate complexes: An efficient and magnetically recoverable nanocatalyst. *New J. Chem.* 43, 12283–12291. doi:10.1039/c9nj01160a
- Norouzi, M., Elhamifar, D., and Abaezadeh, S. (2020). Magnetic ethyl-based mesoporous organosilica composite supported IL/Mn: A novel and highly recoverable nanocatalyst for preparation of 4H-pyrans. *Appl. Surf. Sci. Adv.* 2, 100039. doi:10.1016/j.apsadv.2020.100039
- Pandit, K. S., Chavan, P. V., Desai, U. V., Kulkarni, M. A., and Wadgaonkar, P. P. (2015). Tris-hydroxymethylaminomethane (THAM): A novel organocatalyst for an environmentally benign synthesis of medicinally important tetrahydrobenzo [b] pyrans and pyran-annulated heterocycles. *New J. Chem.* 39, 4452–4463. doi:10.1039/c4nj02346c
- Puangnam, M., and Unob, F. (2008). Preparation and use of chemically modified MCM-41 and silica gel as selective adsorbents for Hg (II) ions. *J. Hazard. Mater.* 154, 578–587. doi:10.1016/j.jhazmat.2007.10.090
- Purbia, R., and Paria, S. (2016). A simple turn on fluorescent sensor for the selective detection of thiamine using coconut water derived luminescent carbon dots. *Biosens. Bioelectron.* 79, 467–475. doi:10.1016/j.bios.2015.12.087
- Qiu, P., Kang, K., Kim, K., Li, W., Cui, M., and Khim, J. (2015). Facile synthesis of uniform yolk-shell structured magnetic mesoporous silica as an advanced photo-Fenton-like catalyst for degrading rhodamine B. *RSC Adv.* 5, 96201–96204. doi:10.1039/c5ra15693a
- Tsuji, K., Jones, C. W., and Davis, M. E. (1999). Organic-functionalized molecular sieves (OFMSs): I. Synthesis and characterization of OFMSs with polar functional groups. *Microporous Mesoporous Mater.* 29, 339–349. doi:10.1016/s1387-1811(99)00003-7
- Vartuli, J., Roth, W., Beck, J., McCullen, S., and Kresge, C. (1998). "The synthesis and properties of M41S and related mesoporous materials," in *Synthesis* (Berlin, Germany: Springer).
- Vartuli, J., Schmitt, K., Kresge, C., Roth, W., Leonowicz, M., McCullen, S., et al. (1994). Development of a formation mechanism for M41S materials. *Stud. Surf. Sci. Catal.* 84, 53–60. doi:10.1016/S0167-2991(08)64096-3
- Veysipour, S., Nasr-Esfahani, M., Rafiee, Z., and Eftekhari Far, B. (2021). Fe₃O₄@ SiO₂@ IL-PVP magnetic nanoparticles: Effective synthesis of spirooxindoles. *Iran. J. Catal.* 11, 125–136.
- Wang, Y.-X., Yang, J., Chou, S.-L., Liu, H. K., Zhang, W.-X., Zhao, D., et al. (2015). Uniform yolk-shell iron sulfide-carbon nanospheres for superior sodium-iron sulfide batteries. *Nat. Commun.* 6, 8689. doi:10.1038/ncomms9689
- Xie, J., Tong, L., Su, L., Xu, Y., Wang, L., and Wang, Y. (2017). Core-shell yolk-shell Si@ C@ Void@ C nanohybrids as advanced lithium ion battery anodes with good electronic conductivity and corrosion resistance. *J. Power Sources* 342, 529–536. doi:10.1016/j.jpowsour.2016.12.094
- Yang, Y., Zhang, W., Zhang, Y., Zheng, A., Sun, H., Li, X., et al. (2015). A single Au nanoparticle anchored inside the porous shell of periodic mesoporous organosilica hollow spheres. *Nano Res.* 8, 3404–3411. doi:10.1007/s12274-015-0840-9
- Yin, Y., Rioux, R. M., Erdonmez, C. K., Hughes, S., Somorjai, G. A., and Alivisatos, A. P. (2004). Formation of hollow nanocrystals through the nanoscale Kirkendall effect. *Science* 304, 711–714. doi:10.1126/science.1096566
- Yu, L., Pan, P., Zhang, Y., Zhang, Y., Wan, L., Cheng, X., et al. (2019). Nonsacrificial self-template synthesis of colloidal magnetic yolk-shell mesoporous organosilicas for efficient oil/water interface catalysis. *Small* 15, 1805465. doi:10.1002/sml.201805465
- Zhang, L., Qiao, S., Jin, Y., Chen, Z., Gu, H., and Lu, G. Q. (2008). Magnetic hollow spheres of periodic mesoporous organosilica and Fe₃O₄ nanocrystals: Fabrication and structure control. *Adv. Mater.* 20, 805–809. doi:10.1002/adma.200700900
- Zhang, Q., and Lee, I. (2013). Core-shell nanostructured catalysts. *Acc. Chem. Res.* 46, 1816–1824. doi:10.1021/ar300230s
- Zhao, X., Sánchez, B. M., Dobson, P. J., and Grant, P. S. (2011). The role of nanomaterials in redox-based supercapacitors for next generation energy storage devices. *Nanoscale* 3, 839–855. doi:10.1039/c0nr00594k
- Zolfigol, M. A., Tavasoli, M., Moosavi-Zare, A. R., Moosavi, P., Kruger, H. G., Shiri, M., et al. (2013). Synthesis of pyranopyrazoles using isonicotinic acid as a dual and biological organocatalyst. *RSC Adv.* 3, 25681–25685. doi:10.1039/c3ra45289a